Azamacrocycles and the azaoxacryptand 4,7,13,16,21,24-hexaoxa-1,10-diazabicyclo[8.8.8]hexacosane as structure-directing agents in the synthesis of microporous metalloaluminophosphates†‡

Martin J. Maple,[a] Eilidh F. Philp,[a] Alexandra M. Z. Slawin,[a] Philip Lightfoot,[a] Paul A. Cox[b] and Paul A.Wright*[a]

[a]School of Chemistry, University of St Andrews, Purdie Building, North Haugh, St Andrews, Fife, UK KY16 9ST
[b]Centre for Molecular Design, University of Portsmouth, King Henry Building, King Henry I Street, Portsmouth, Hants, UK PO1 2DY

Hydrothermal syntheses of aluminophosphates have been performed in the presence of Mg^{2+}, Cr^{3+}, Mn^{2+}, Fe^{2+}, Co^{2+}, Ni^{2+}, Cu^{2+} and Zn^{2+} cations using the macrocycles 1,4,7-trimethyl-1,4,7-triazacyclononane (tmtacn), 1,4,8,11-tetraazacyclotetradecane (cyclam), 1,4,8,11-tetramethyl-1,4,8,11-tetraazacyclotetradecane (tmtact) and 1,4,7,10,13,16-hexamethyl-1,4,7,10,13,16-hexaazacyclooctadecane (hmhaco), and the cryptand 4,7,13,16,21,24-hexaoxa-1,10-diazabicyclo[8.8.8]hexacosane (K222) as structure directing agents. Tmtacn is found to template MAPO-18, K222 to template MAPO-42 and tmtact to template STA-6 or STA-7; the solids formed using tmtact depend on the metal cation present. Use of cyclam with a cobalt aluminophosphate gel results in a new solid, $Co^{II}(C_{10}N_4H_{24})Al(PO_4)PO_3(OH)$, which consists of aluminophosphate chains of stoichiometry AlP_2O_8H linked *via* cobalt–cyclam complexes. Bonding between the cobalt–cyclam complexes and the aluminophosphate chains is through direct Co–O bonds and a complex hydrogen-bonding network—quite different from that between the three-dimensionally connected frameworks and the tertiary amine-containing templates. An isostructural solid is formed *via* the substitution of cobalt by nickel in the aluminophosphate gel. The role of divalent cations in structure direction, in the presence of tertiary amine-containing macrocycles, has been further investigated. Adding Co^{2+} or Zn^{2+}, in particular, enhances the amines' ability to act as templates for STA-7 and MAPO-42, yet single crystal and powder diffraction using synchrotron radiation indicates that the divalent cations do not remain within the macrocycles after crystallisation.

Introduction

The incorporation of functional organic molecules within open framework solids offers promise of inorganic–organic hybrid materials, such as encapsulated laser dye molecules in inorganic hosts,[1] solids with non-linear optical properties,[2] cation exchangers with novel selectivities, proton conductors and 'ship-in-a-bottle' catalysts.[3–5] If such functional molecules are included during synthesis, there is no need to calcine the solids to obtain open pores, with the consequent destruction of expensive templates, attendant safety concerns and the possibility of associated structural breakdown. Our own results on the incorporation of 1,4,8,11-tetramethyl-1,4,8,11-tetraaza-cyclotetradecane (tmtact) into the novel solids STA-6[6] and STA-7[7] (the latter is also formed in the presence of 1,4,7,10,13,16-hexamethyl-1,4,7,10,13,16-hexaazacyclooctade-cane (hmhaco) and cobalt or zinc), together with those on the incorporation of the oxaazacryptand 4,7,13,16,21,24-hexaoxa-1,10-diazabicyclo[8.8.8]hexacosane (K222) and related aza-crown ethers into AlPO₄-42,[8,9] and of porphyrins into VPI-5,[10] have demonstrated that azamacrocycles and cryptands may be included, unbound, within aluminophosphate-based solids. By extrapolation from the properties associated with macrocycles, such systems should possess exciting cation complexing and catalytic potential.

We have already shown that, in the presence of tmtact and the divalent metal cations Mg^{2+}, Mn^{2+} or Fe^{2+}, the cage structure STA-6 is formed, whereas, in the presence of Co^{2+} or Zn^{2+}, the STA-7 structure results.[7] In the first part of this paper we explore further the compositional range of solids that may be prepared using tmtact as a template and examine the effect of using mixtures of divalent cations in the syntheses. We also compare these structures with those formed using the unsubstituted azamacrocycle cyclam under similar conditions.

In the second part of this work, we investigate (a) the use of the related methyl-substituted azamacrocycle, 1,4,7-trimethyl-1,4,7-triazacyclononane (tmtacn), in similar metalloalumino-phosphate preparations, and (b) whether the cryptand K222 will give aluminophosphate-based solids with the AlPO₄-42 structure in the presence of a range of divalent cations. It is known that although AlPO₄-42 is formed in the presence of K222 as the only additive, co-addition of tetramethylammo-nium and fluoride ions to the gels result in products which are more crystalline. In these materials, K222, tetramethylammo-nium ions and fluoride ions occupy sites in the α-cage, sodalite cage and double four-membered ring units of the structure, respectively.[11]

The molecular structures of cyclam, tmtacn, tmtact, hmhaco and K222 are shown in Scheme 1 as **1** to **5**, respectively.

Our molecular modelling studies[7] of protonated templates within STA-6 and STA-7 showed that only tmtact (and not hmhaco) can fit within the cages of STA-6, so that STA-6 is not templated by the larger macrocycle. Both tmtact and hmhaco are able to fit within the larger of the two types of cage in STA-7, giving this solid in the presence of cations that are expected
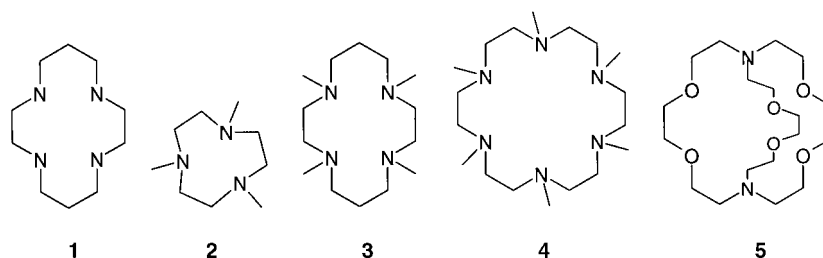
Scheme 1

to be strongly complexed (such as Co^{2+} and Zn^{2+}). There is no evidence that the cations remain complexed in the macrocycle after crystallisation of STA-6 and STA-7—instead they end up in the tetrahedral sites of the aluminophosphate framework.[7] In this investigation we have performed similar modelling studies to understand the action of tmtacn and K222.

Experimental

Homogeneous gels in a range of compositions were made up from mixtures of orthophosphoric acid solution, metal salts (usually acetates), hydrated aluminium hydroxide (Aldrich) and the azamacrocycles cyclam, tmtacn, tmtact, hmhaco or the cryptand K222 (Aldrich). Details of the gel compositions are given in Table 1, along with others that have been reported previously. In each case, the initial pH was adjusted to 7 by addition of the appropriate amount of base (azamacrocycle or cryptand). This required base/P ratios of between 0.4 and 0.7, depending on the amount of metal salt added. Gels were introduced into PTFE-lined stainless steel autoclaves and heated at 190 °C for 48 h. Crystalline products were separated from the resulting suspensions by sonication, filtered, washed with distilled water and dried in air.

X-Ray powder diffraction patterns of all products were collected (using Cu-Kα radiation) to enable phase identification. For samples containing manganese, iron or cobalt, X-ray fluorescence from the Cu-Kα radiation results in a high background signal. To circumvent this problem, selected samples were studied using synchrotron X-radiation monochromated to a wavelength of 0.99555(1) Å on station 9.1 at the SRS at Daresbury, or using a laboratory diffractometer equipped with Fe-Kα₁ X-radiation. Where crystals of sufficient quality were available, they were examined by single crystal diffractometry, either using an in-house diffractometer or at

Table 1 Gel compositions used in this work and others reported previously. The products obtained from hydrothermal syntheses performed with these gels are reported, along with product phase identification from X-ray powder diffractometry and NMR spectroscopic and chemical analysis of selected materials[a]

Cation ratio in synthesis gel	Azamacro-cycle (R)	Product, by XRD and optical examination	NMR, δ_c values for amines extracted by acid treatment	Inorganic composition (from EDX and ICP-AES)[b]	Reference
0.2Mg:0.8Al:1.0P	cyclam	unidentified			This work
0.2Co:0.8Al:1.0P	cyclam	CoAPO-cyclam-1		$CoAlP_2O_8H \cdot C_{10}N_4H_{24}$	This work
0.2Ni:0.8Al:1.0P	cyclam	NiAPO-cyclam-1			This work
0.15Mg:0.85Al:1.0P	tmtacn	MgAPO-18[c]		$Mg_{0.15}Al_{0.85}PO_4$	This work
0.15Co:0.85Al:1.0P	tmtacn	CoAPO-18[c]			This work
1.0Al:1.0P	tmtact	AlPO₄-21[d]			Ref. 6
0.2Mg:0.8Al:1.0P	tmtact	Mg-STA-6[e]	51.9, 47.0, 45.3, 19.5	$Mg_{0.2}Al_{0.8}PO_4$	Ref. 6
0.2Cr:0.8Al:1.0P	tmtact	AlPO₄-21[d]	37.4		This work
0.2Mn:0.8Al:1.0P	tmtact	Mn-STA-6[e]		$Mn_{0.2}Al_{0.8}PO_4$	Ref. 7
0.2Fe:0.8Al:1.0P	tmtact	Fe-STA-6[e]			Ref. 7
0.2Co:0.8Al:1.0P	tmtact	Co-STA-7[f]	51.9, 47.0, 45.3, 19.6		Ref. 7
0.2Ni:0.8Al:1.0P	tmtact	unidentified			This work
0.2Cu:0.8Al:1.0P	tmtact	AlPO₄-21[d]			This work
0.2Zn:0.8Al:1.0P	tmtact	Zn-STA-7[f]	37.4 + 51.9, 47.0, 45.3, 19.6		Ref. 7
0.0625Zn:0.1875Mg:0.75Al:1.0P	tmtact	STA-6[e] + STA-7[f]			This work
0.125Zn:0.125Mg:0.75Al:1.0P	tmtact	STA-7[f]			This work
0.1875Zn:0.065Mg:0.75Al:1.0P	tmtact	STA-6[e] + STA-7[f]			This work
1.0Al:1.0P	hmhaco	AlPO₄-21[d]	53.2, 47.0, 46.1, 36.1		Ref. 7 and this work
0.2Mg:0.8Al:1.0P	hmhaco	MgAPO-36[g] + Mg-STA-7[f]	53.9, 53.1, 49.8, 45.9, 45.4		Ref. 7
0.2Fe:0.8Al:1.0P	hmhaco	AlPO₄-21[d]			This work
0.2Co:0.8Al:1.0P	hmhaco	Co-STA-7[f]	53.2, 44.8	$Co_{0.2}Al_{0.8}PO_4$	Ref. 7
0.2Mg:0.8Al:1.0P	K222	MgAPO-5[h] + MgAPO-42[i]			This work
0.2Mn:0.8Al:1.0P	K222	MnAPO-5[h] + MnAPO-42[i]			This work
0.2Fe:0.8Al:1.0P	K222	FeAPO-5[h] + FeAPO-42[i]			This work
0.2Co:0.8Al:1.0P	K222	CoAPO-42[i] + CoAPO-5[h]			This work
0.2Zn:0.8Al:1.0P	K222	ZnAPO-42[i]		$Zn_{0.2}Al_{0.8}PO_4$	This work

[a]The ratio R/P in the gel was varied from 0.4–0.7, so that the gel pH was always initially 7; a typical gel composition is $0.2MOAc_2 \cdot 4H_2O:0.8Al(OH)_3 \cdot xH_2O:H_3PO_4:400H_2O:0.5R$. [b]The cation contents of the solids CoAPO-cyclam-1, MgAPO-18, Mg-STA-6, Mn-STA-6 and ZnAPO-42 were determined using EDX, and the composition of Co-STA-7 was determined by ICP-AES. [c]IZA structure type code: AEI [d]IZA structure type code: AWO. [e]SAS. [f]SAV. [g]ATS. [h]AFI. [i]LTA.

the microcrystal diffraction station 9.8 at Daresbury, depending on the crystal size.

For selected crystalline products, in order to determine whether the azamacrocycles had been incorporated intact, the inorganic framework was dissolved in 5 M HCl and the liberated amines analysed by NMR spectroscopy according to published procedures.[7] ^{13}C NMR spectra were recorded at 75 MHz on a Bruker AM300 instrument using sodium 3-trimethylsilylpropane sulfonate as the reference. Solid state ^{13}C MASNMR analysis was also performed on Mg-STA-6 and Zn-STA-7.

To model the likely position of templates within microporous solids we adopted the conventional computational approach of combining Monte Carlo docking and subsequent simulated annealing, reported elsewhere.[7] Calculations were performed using constant valence forcefield (CVFF) within the program Discover,[12] assuming that short-range interactions between the framework and the template molecules will determine the favoured locations, rather than Coulombic forces.

To confirm the presence of metal cations within selected samples, single crystals were studied by energy dispersive X-ray (EDX) analysis (carried out on a Jeol JEM-2010 electron microscope using an Oxford Instruments EDX attachment) and powders were examined using inductively coupled plasma-atomic emission spectroscopy (ICP-AES) on samples dissolved in nitric acid.

Results

The results of the hydrothermal syntheses performed in this work and those previously reported are given in Table 1, including phase identification according to X-ray powder diffractometry and analysis of selected materials by NMR spectroscopy and chemical analysis.

Templating with tmtact and hmhaco

Use of tmtact as a template was known to produce either STA-6 or STA-7 (structure types SAS and SAV, respectively), depending on the divalent cation used (Mg^{2+}, Mn^{2+} or Fe^{2+} result in STA-6, Co^{2+} or Zn^{2+} give STA-7).[7] Synchrotron X-ray powder diffraction profiles of the as-prepared solids synthesised with Mn^{2+}, Fe^{2+} or Co^{2+} were obtained. MnAPO and CoAPO samples only give diffraction peaks due to STA-6 and STA-7, respectively, whereas the FeAPO
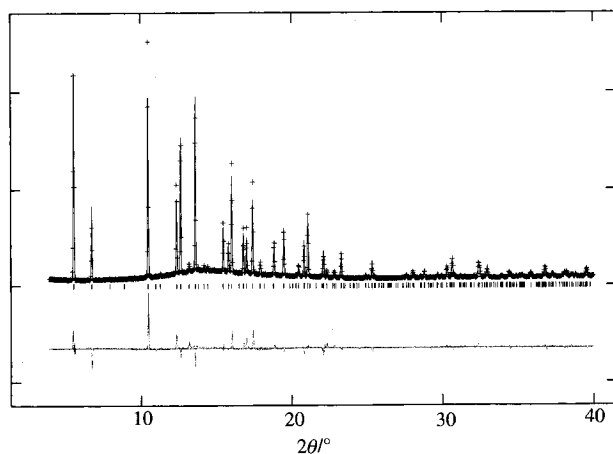

Fig. 1 Rietveld refinement of the X-ray powder diffraction profile of Mn-STA-6, collected using synchrotron X-rays [$\lambda = 0.99555(1)$ Å] at 293 K. Mn-STA-6 has space group symmetry $P4/mnc$, with $a = 14.2727(3)$, $c = 10.3750(3)$ Å. Tmtact template is included in the model in positions calculated by molecular modelling, and statistically disordered.
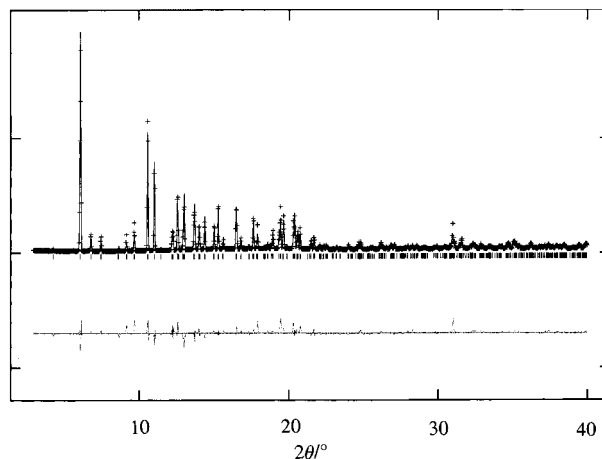
Fig. 2 Rietveld refinement of the X-ray powder diffraction profile of Co-STA-7, collected using synchrotron X-rays [$\lambda = 0.99555(1)$ Å] at 293 K. Co-STA-7 has space group symmetry $P4/n$, with $a = 18.640(2)$, $c = 9.3755(7)$ Å. Tmtact template is included in the model in positions calculated by molecular modelling, and statistically disordered.

sample is mainly STA-6 with traces of STA-7. The Rietveld refinements of the Mn-STA-6 and Co-STA-7 are shown in Fig. 1 and 2 and confirm the solids are phase pure. (See the Crystallography section for details of the refinements.) Attempts to prepare STA-6 or STA-7 with nickel, copper, or chromium cations were unsuccessful. For chromium and copper-containing gels, the only crystalline phase to form is $AlPO_4$-21, whereas nickel-containing gels give unidentified phases that are bright salmon pink.

In order to examine further the role of the divalent cations in controlling the syntheses, a cobalt-containing gel was seeded with Mg-STA-6 crystals. In other aluminophosphate-based preparations, this approach can be used to favour the crystallisation of one phase over another that can co-crystallise from the gel. In this case, however, Co-STA-7 is formed. In addition, mixtures of Mg^{2+} and Zn^{2+} in different ratios were used in a series of experiments. For preparations with $Zn^{2+} : Mg^{2+}$ ratios of 25:75 and 50:50, the product is a physical mixture of STA-6 and STA-7, the amount of STA-7 increasing as the zinc content increases. For a $Zn^{2+} : Mg^{2+}$ ratio of 75:25, only STA-7 is observed. ^{13}C NMR studies of selected systems indicate that whereas STA-6 contains only intact tmtact, STA-7 contains tmtact as well as other amine fragments, presumably in the smaller of the two different types of cage present in the structure. Aluminophosphate $AlPO_4$-21 does not contain tmtact intact: the NMR signal observed from organics liberated from $AlPO_4$-21 prepared in the presence of tmtact (δ_c 37.4) is consistent with included dimethylammonium ions. Syntheses using hmhaco in the presence of Mg^{2+}, Mn^{2+}, Co^{2+} or Zn^{2+} demonstrate that only those preparations including Co^{2+} or Zn^{2+} result in pure STA-7, the other preparations giving mainly MAPO-5, MAPO-36 and $AlPO_4$-21.

'Templating' with cyclam

Addition of cyclam to a cobalt aluminophosphate preparation for comparison gave crystals of a novel phase that was identified by single crystal diffraction (CoAPO-cyclam-1; see Crystallography section). The structure of this phase can be described in terms of aluminophosphate chains, of stoichiometry AlP_2O_8H, running parallel to the crystallographic *a*-axis. These chains are connected to four other chains *via* P–O–Co–O–P linkages, with the cobalt being complexed within the cyclam rings (see Fig. 3). Within the chains, aluminium is tetrahedrally coordinated by oxygens that are in turn linked to tetrahedrally coordinated phosphorus atoms. Of the four
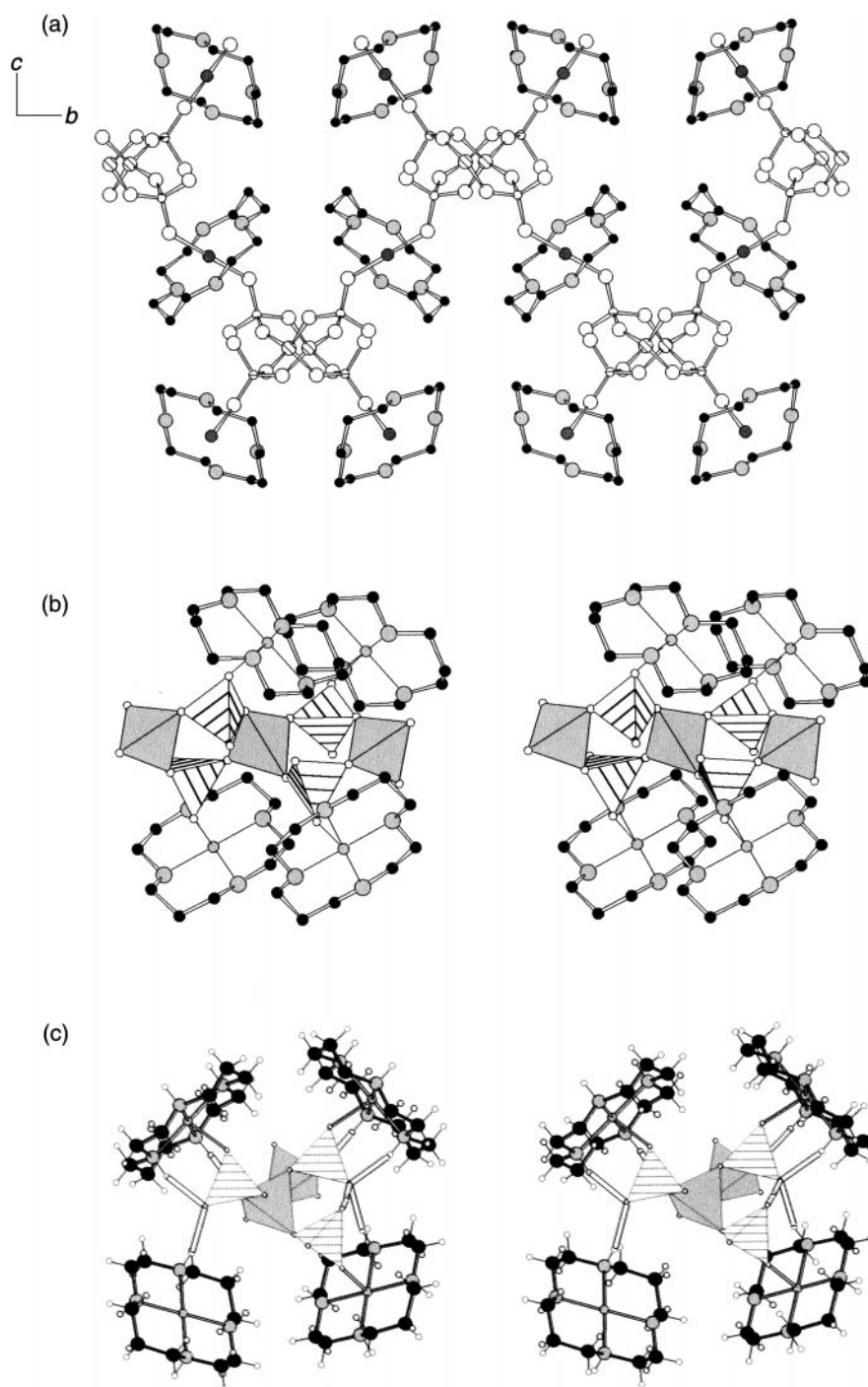
Fig. 3 Views of CoAPO-cyclam-1. (a) Down the crystallographic *c*-axis, along the AlP_2O_8H chains. (b) Stereoview of a section of the structure, showing the arrangement of Co-cyclam units linked *via* Co–O bonds to the phosphate oxygens of the aluminophosphate chains. C atoms are represented by black spheres, N atoms by grey spheres, Co by smaller grey spheres and PO_4 and AlO_4 tetrahedra are hatched and grey, respectively. Hydrogens are omitted for clarity. (c) Stereoview including the hydrogen atoms and also indicating the location of hydrogen bonds within the structure.

oxygens surrounding each of the two crystallographically distinct phosphorus atoms, two are involved in P–O–Al linkages and one in a P–O–Co link, leaving one in each PO_4 tetrahedron apparently attached only to one phosphorus. As described in the Crystallography section, these are P–O single bonds, the oxygens of which are hydrogen bonded to each other (with an O–O distance of 2.50(1) Å) and to nitrogens of the cyclam units, to give a compound of formula $Co^{II}(C_{10}N_4H_{24})Al(PO_4)PO_3(OH)$. Fig. 3c shows the H-bonding network, with hydrogens on the cyclam nitrogens H-bonding to oxygens of the aluminophosphate chain with (N)H–O bond distances of 2.04(1), 2.06(1), 2.29(2) and

2.69(2) Å. Replacing cobalt by nickel in the synthesis gel gave a purple solid which is thought to be isostructural with CoAPO-cyclam-1 on the basis of its powder X-ray diffraction pattern. Replacing cobalt by magnesium gave a different, unidentified, phase.

Templating with tmtacn

Addition of tmtacn to the reaction gel results in the preparation of the known MAPO-18 (AEI) structure type. Crystals of MgAPO-18 ($60 \times 40 \times 35$ μm) of suitable quality for microcrystal diffraction were prepared; the results of such an analysis
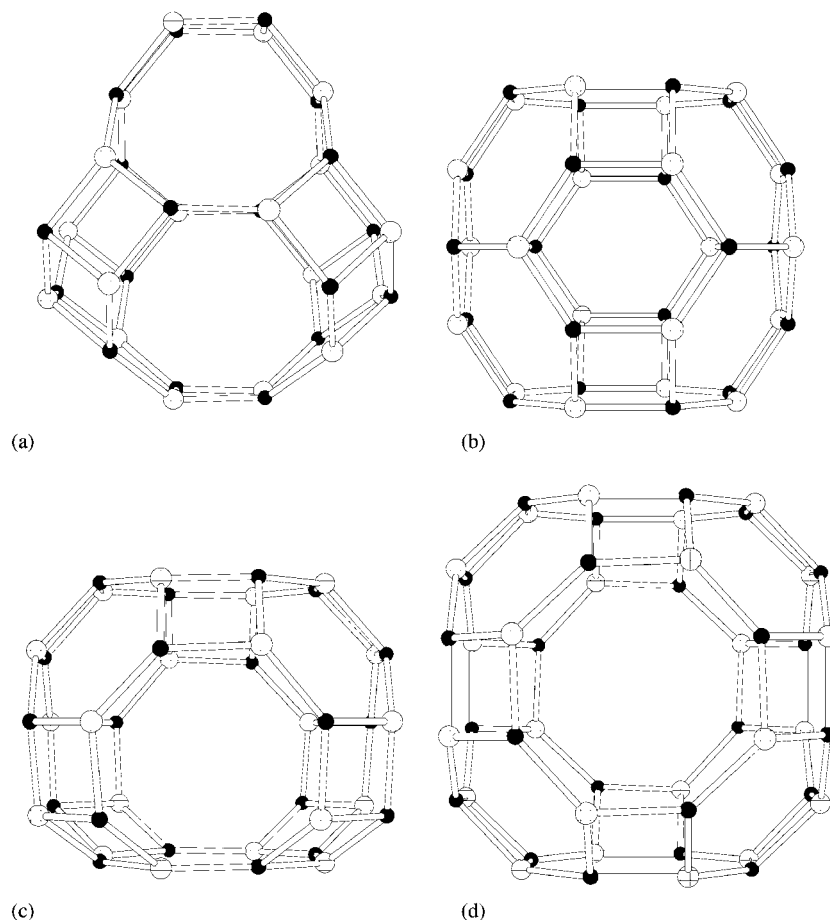
(a)

(b)

(c)

(d)

Fig. 4 Comparison of the cages present in the framework structures of (a) MAPO-18, (b) STA-6, (c) STA-7 and (d) AlPO$_4$-42. Only the positions of tetrahedrally coordinated framework cations are marked.

are described in the Crystallography section. Selected single crystals were analysed by EDX and found to contain magnesium, with a Mg/P ratio of *ca.* 0.15; TGA showed there to be 2.6 tmtacn molecules per unit cell (an occupancy of 65%). Like AlPO$_4$-42, STA-6 and STA-7, MAPO-18 has a small pore structure that may be considered as possessing pore space made up entirely of cages. The cage, which is connected to six other identical cages by 8MR windows, is compared with the cages from the other structures in this work in Fig. 4. Molecular modelling reveals a strong preference of the uncharged tmtacn template for a site that possesses pseudo-threefold symmetry (Fig. 5). Since it is possible that the macrocycle could be incorporated in a monoprotonated form to balance the negative charge imparted to the framework by the incorporation of magnesium, the modelling was also performed for this case. The final energy-minimised position is very close to that of the neutral amine. Inclusion of the

template in this site at a refined occupancy level of 2.8 per 4 cages in the unit cell gives a marked improvement in the fit to the single crystal diffraction data, reducing R(obs) from 13.0 to 8.4% (see Crystallography section).

Templating with K222

The use of K222 as a template for MAPOs follows a clear trend. Whereas Mg^{2+}, Mn^{2+} or Fe^{2+} gives MAPO-42 as a minor product along with MAPO-5, syntheses with cobalt and, in particular, zinc cations gave highly crystalline MAPO-42, which is phase pure in the case of ZnAPO-42. TGA reveals there are *ca.* 8 K222 molecules per unit cell which corresponds to one molecule per supercage. Molecular modelling indicates that whereas the fit of the K222 cryptand within the supercage (α-cage) of the structure is energetically favourable, there is no uniquely favoured position. Modelled scattering from disordered template molecules that fully occupy the α-cages significantly improves the single crystal refinement residual R(obs) from 14.9 to 12.3%. The refinement also shows conclusively that zinc does not reside within the cryptand in the structure.

Crystallography

Bulk microcrystalline samples of as-prepared Mn-STA-6, Fe-STA-6 and Co-STA-7 were examined by room temperature powder diffraction at station 9.1 of the Daresbury synchrotron to circumvent difficulties due to fluorescence. Data were collected using monochromated X-rays of wavelength 0.99555(1) Å over the 2θ range 3–60°, with a step size of 0.02°. The powder profiles were matched using the Rietveld refinement technique in the GSAS suite of programs.[13] The atomic coordinates derived from single crystal diffraction at
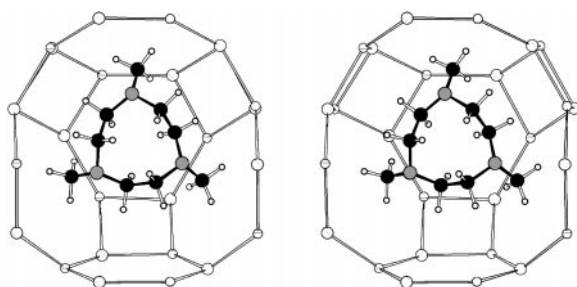

Fig. 5 Diagrammatic representation (stereoview) of the minimum energy position of tmtacn. The molecule's threefold axis matches well with the pseudo-threefold axis of the portion of framework that makes up part of the MAPO-18 cage. For clarity, only the position of tetrahedral atoms in the framework are shown.

150 K for STA-6, and at room temperature for STA-7, were used as starting models. Template positions derived from modelling studies were input with large temperature factors ($U = 0.3$) and the templates permitted to exhibit statistical disorder over symmetrically equivalent positions. The fractional occupancy of the template was permitted to refine within experimentally reasonable limits. The fractional coordinates of the framework were also permitted to undergo constrained refinement. For Mn-STA-6, the structure was refined in space group $P4/mnc$ [$a = 14.2727(3)$, $c = 10.3750(3)$ Å] with final goodness-of-fit indices of $R_{wp} = 9.48$, $R_p = 6.66\%$. For Co-STA-7 the structure was refined in $P4/n$ [$a = 18.640(2)$, $c = 9.3755(7)$ Å] with the final indices $R_{wp} = 15.99$, $R_p = 11.33\%$ (Fig. 1 and 2).

The single crystals of CoAPO-cyclam-1 obtained were large enough (up to 0.3 mm in dimensions) to be studied on a laboratory diffractometer. The structure was solved and refined using SHELX and SHELXL, respectively.[14] The positions of the aluminophosphate chain and the cyclam molecules were determined directly. Hydrogens were placed on the carbon atoms in idealised geometries and were refined with $U(H) = 1.2U(C)_{eq}$. Hydrogen atoms on the cyclam nitrogens were constrained to lie at a distance of 0.98 Å from N, and were allowed to refine isotropically to positions that indicate a hydrogen bonding interaction with oxygens of the aluminophosphate chain. Finally, a proton was found to lie between the two oxygens on the phosphorus atoms that do not bridge to aluminium or cobalt. This proton was placed 0.98 Å from one of these oxygens and refined to 1.53(1) Å from the other one, indicating a strong hydrogen-bond. Al–O and P–O bond lengths were within the expected range for tetrahedrally coordinated cations with single bonds to oxygen (Al–O 1.73–1.75, P–O 1.48–1.55 Å) and each of two distinct cobalt cations was found to be octahedrally coordinated by four nitrogens and two oxygens, with Co–N bond lengths of between 2.102(3) and 2.114(3) Å and Co–O bond lengths of 2.089(2) and 2.122(2) Å. Further crystallographic details are given at the end of this section.

CCDC 1145/228. See http://www.rsc.org/suppdata/jm/b0/b003430o/ for crystallographic files in .cif format.

Single microcrystals of MgAPO-18 and ZnAPO-42 were examined on station 9.8 at the Daresbury synchrotron. In each case, the basic framework structure was solved using SIR92[15] and refined using the teXsan suite of programs,[16] and shown to possess the same space group and framework structure as reported previously[17] for AlPO$_4$-18 and AlPO$_4$-42. For MgAPO-18, putting the tmtacn template into the position suggested by the molecular modelling significantly improves the goodness-of-fit, R(obs) decreasing from 13.0 to 8.4%, and for ZnAPO-42, inputting the disordered template improves R(obs) from 14.9 to 12.3%. Attempts to locate zinc cations within the cryptand in ZnAPO-42 (at 0.25, 0.25, 0.25) showed that there was none. In each case, average bond lengths and refined scattering on the 'Al' sites indicate that divalent metal substitution has occurred into those sites. For MgAPO-18, the (Mg,Al)–O average bond length is 1.76(1) Å, and for ZnAPO-42, the (Zn,Al)–O average bond length is 1.75(2) Å. Further crystallographic details are given below.

Crystal data

Note that the crystallographic programs SHELX and teXsan refine on F^2 and F, respectively. The compositions are those consistent with template occupancies derived from the single crystal data refinements.

CoAPO-cyclam-1. Co^{II}(C$_{10}$N$_4$H$_{24}$)Al(PO$_4$)PO$_3$(OH), $M = 477.19$, monoclinic, $a = 14.978(1)$, $b = 14.720(1)$,

$c = 8.479(1)$ Å, $\beta = 98.323(1)°$, $U = 1849.8(2)$ Å^3, $T = 293$ K, space group $P2_1/c$ (no. 14), $Z = 4$, μ(Mo-Kα) = 1.195 mm^{-1}, 7991 reflections measured, 2659 unique, of which 2100 were observed. The final R(obs) was 2.9% with R_{all} of 4.4%.

MAPO-18. [(Mg,Al)$_3$P$_3$O$_{12}$·0.35(N$_3$C$_9$H$_{21}$)], $M = 426$, monoclinic, $a = 13.795(3)$, $b = 12.830(3)$, $c = 18.815(5)$ Å, $\beta = 89.959(7)°$, $U = 3330$ Å^3, $T = 150$ K, space group $C2/c$ (no. 15), $Z = 8$, μ(0.694 Å) = 0.567 mm^{-1}, 11252 reflections measured, 4501 unique, of which 2535 were observed. The final R(obs) was 8.4% with $wR_F = 10.6\%$. Note that for MgAPO-18, the refinement was performed using a purely aluminophosphate model, because the scattering of magnesium and aluminium are so similar.

ZnAPO-42. [Zn$_{0.2}$Al$_{0.8}$PO$_4$·0.083(N$_2$C$_{18}$O$_6$H$_{38}$)], $M = 158.0$, cubic, $a = 23.990(8)$ Å, $U = 13806(6)$ Å^3, $T = 150$ K, space group $Fm\bar{3}c$ (no. 226), $Z = 96$, μ(0.694 Å) = 1.34 mm^{-1}, 6420 reflections measured, 1007 unique, of which 312 were observed. The final R(obs) was 12.3% with $wR_F = 13.3\%$.

Discussion

Azamacrocycles containing tertiary nitrogen atoms and the azaoxacryptand K222 have been shown to be effective templates for the synthesis of open framework metalloaluminophosphates, where they are included, unbound, in cages within the structures of MAPO-18, STA-6, STA-7 and MAPO-42. By contrast, cyclam itself, with four secondary nitrogen atoms within the ring, remains coordinated to cobalt in the final product under similar conditions, where the macrocycle becomes an integral part of the structure. The latter kind of behaviour is similar to that observed in the cyclam-containing gallium phosphates reported previously.[18] The aluminophosphate chain is similar to that identified previously[19,20] and proposed by Ozin et al. to be the progenitor to very many of the aluminophosphate structures.[21] Hydrogen-bonding between the cyclam and the aluminophosphate chain and within the chain itself are important structural features that are distinctly different from the bonding observed between template molecules that possess tertiary amine groups and three-dimensionally connected frameworks. Presumably, the ability of the secondary amine hydrogen atoms to hydrogen bond to phosphate group oxygens crucially directs the synthesis of CoAPO-cyclam-1 (and the related nickel-containing structure).

Evidence from X-ray diffraction and sample colour indicate that in the MAPOs containing tmtacn, tmtact, hmhaco and K222 the divalent metal cations do not remain complexed within the macrocycle after crystallisation. For example, no X-ray scattering was observed in the centre of the K222 cryptand in ZnAPO-42 (the site refined to zero occupancy) and crystallites containing tmtact and cobalt were blue before, and green after, calcination, which is consistent with the oxidation of cobalt from 2+ to 3+ within the tetrahedral sites in the framework.[22] This indicates that the cations are tetrahedrally coordinated within the framework rather than remaining complexed within the macrocyclic ligand and implies that they are more strongly bound within the framework.

The role of divalent cations in directing the syntheses of microporous metalloaluminophosphates using tmtact has been investigated further. In the presence of divalent cations that are expected to be more weakly bound within the macrocycle (Mg^{2+}, Fe^{2+}, Mn^{2+}), STA-6 is also produced, whereas in the presence of cobalt and zinc cations, STA-7 is formed. Where aliovalent substitution is not possible (i.e. in pure aluminophosphate or Cr^{3+}-containing aluminophosphate gels), the AlPO$_4$-21 structure type results, and intact macrocycle is not incorporated. The synthesis of Co-STA-7 is not affected by the presence of Mg-STA-6 seeds and, furthermore, syntheses

from gels containing mixtures of Mg^{2+} and Zn^{2+} give mixtures of STA-6 and STA-7. Parallel studies using hmhaco reveal that only in the presence of cobalt or zinc cations does it act to template STA-7. Finally, it is found that, although some MAPO-42 is prepared in the presence of K222 when M is Mg^{2+}, Mn^{2+} or Fe^{2+}, the cations Co^{2+} and Zn^{2+} greatly enhance the yield, and ZnAPO-42 is readily prepared phase pure in this way. In summary, it is clear that the type of cations present together with tmtact, hmhaco and K222 have a decisive influence on the nature of the product, without remaining within the macrocycle upon crystallisation. It seems likely that the more strongly bound metal cations could be retained within the macrocycle during the initial stages of nucleation and crystal growth, and control the shape of the complex during its incorporation.

Acknowledgements

References

1 G. Ihlein, F. Schuth, O. Krauss and U. Vietzeand F. Laeri, *Adv. Mater.*, 1998, **10**, 1117.
2 I. Bull, L. A. Villaescusa, S. J. Treat, M. A. Camblor, P. A. Wright, P. Lightfoot and R. E. Morris, *J. Am. Chem. Soc.*, in press.
3 N. Herron, G. D. Stucky and C. A. Tolman, *J. Chem. Soc., Chem. Commun.*, 1986, 1521.
4 M. J. Sabater, A. Corma, V. Fornes and H. Garcia, *Chem. Commun.*, 1997, 1285.
5 J. C. Medina, N. Gabriunas and E. Paez-Mozo, *J. Mol. Catal. A: Chem.*, 1997, **115**, 233.
6 V. Patinec, P. A. Wright, P. Lightfoot, R. A. Aitken and P. A. Cox, *J. Chem. Soc., Dalton Trans.*, 1999, 3909.
7 P. A. Wright, M. J. Maple, A. M. Z. Slawin, V. Patinec, R. A. Aitken, S. Welsh and P. A. Cox, *J. Chem. Soc., Dalton Trans.*, 2000, 1243.
8 L. Schreyeck, F. D'Agosto, J. Stumbe, P. Caullet and J. C. Mougenel, *Chem. Commun.*, 1997, 1241.
9 L. Schreyeck, P. Caullet, J. C. Mougenel and B. Marler, *Proceedings of the 12th International Zeolite Conference*, ed. M. M. J. Treacy, B. K. Marcus, M. E. Bisher and J. B. Higgens, Materials Research Society, Baltimore, 1998, p. 1733.
10 T. A. Khan and J. A. Hriljac, *Inorg. Chim. Acta*, 1999, **294**, 179.
11 L. Schreyeck, J. Stumbe, P. Caullet, J. C. Mougenel and B. Marler, *Microporous Mesoporous Mater.*, 1998, **22**, 87.
12 Discover 3.1 program, MSI, San Diego, CA, 1993
13 A. C. Larson and R. B. von Dreele, Generalized Crystal Structure Analysis System, Los Alamos National Laboratory, USA, 1994.
14 G. M. Sheldrick, SHELX, Program for the solution of crystal structures, University of Göttingen, 1986; G. M. Sheldrick, SHELXTL, version 5.3, Program for the solution of crystal structures, University of Göttingen, 1993.
15 A. Altomare, M. C. Burla, M. Camalli, M. Cascarano, C. Giacovazzo, A. Gugliardi and G. Polidori, *J. Appl. Crystallogr.*, 1993, **26**, 343.
16 teXsan Single Crystal Analysis Software, version 1.6, Molecular Structure Corporation, The Woodlands, TX, USA, 1993.
17 W. M. Meier, D. H. Olson and Ch. Baerlocher, *Atlas of Zeolite Structure Types*, 4th edn., Elsevier, London, 1996; W. M. Meier, D. H. Olson and Ch. Baerlocher, *Zeolites*, 1996, **17**, 1.
18 P. Reinert, J. Patarin and B. Marler, *Eur. J. Solid State Inorg. Chem.*, 1998, **35**, 389; D. S. Wragg, G. B. Hix and R. E. Morris, *J. Am. Chem. Soc.*, 1998, **120**, 6822.
19 R. H. Jones, J. M. Thomas, R. Xu, Q. Huo, Y. Xu, A. K. Cheetham and D. Bieber, *J. Chem. Soc., Chem. Commun.*, 1990, 1170.
20 W. Tieli, Y. Long and P. Wenqin, *J. Solid State Chem.*, 1990, **89**, 392.
21 S. Oliver, A. Kuperman and G. A. Ozin, *Angew. Chem., Int. Ed.*, 1998, **37**, 46.
22 J. M. Thomas, G. N. Greaves, G. Sankar, P. A. Wright, J. Chen, A. J. Dent and L. Marchese, *Angew. Chem., Int. Ed. Engl.*, 1994, **33**, 1871.